58916-00-105, 85088-24-105 April 1991

(INVITED PRESENTATION)

ANL/CP--73158

DE91 014466

FLUX PINNING AND DISSIPATION IN HIGH-TEMPERATURE SUPERCONDUCTORS*

K.E. Gray and D.H. Kim

Materials Science Division
and
Science and Technology Center for Superconductivity

Argonne National Laboratory, Argonne, IL 60439 USA

Invited article to be presented at: International Workshop on HTCS Thin Films: Properties and Applications, April 15-19, 1991, Rome Italy.

jmc

---

*Work supported in part by the U.S. Department of Energy, Division of Basic Energy Sciences-Materials Sciences, under contract #W-31-109-ENG-38, and the National Science Foundation -- Office of Science and Technology Centers under contract #STC-8809854.

FLUX PINNING AND DISSIPATION IN HIGH-TEMPERATURE SUPERCONDUCTORS*

K.E. GRAY and D.H. KIM

Materials Sciences Division, Argonne National Laboratory, Argonne, Illinois, 60439, USA

The effect of anisotropy on the field-induced broadening of resistive transitions in the highly-anisotropic high-temperature superconductors (HTS) is considered. For the applied field, H, *parallel* to the superconducting Cu-O layers the absence of a Lorentz-force, together with intrinsic pinning of the insulating region between layers, leads to an explanation other than flux motion. However, for H parallel to the *c*-axis, the lack of intrinsic pinning implies that the much greater broadening is due to thermally-activated flux motion. We show experimental evidence that the associated flux motion occurs as a result of a crossover from three dimensional (3D) vortex *lines* to 2D independent *pancake-like* vortices, residing in the Cu-O layers. This 3D to 2D crossover occurs when k_BT exceeds the Josephson coupling energy. For $YBa_2Cu_3O_7$, this dimensional crossover does not occur *below* H_{c2}, presumably because the conducting Cu-O chains short circuit the Josephson interlayer coupling.

1. INTRODUCTION

The purpose of this paper is to discuss recent developments in our understanding of transport properties of high-temperature superconductors (HTS), such as the effects of the large anisotropy and fluctuations on critical currents and dissipation[1-5]. Experimental results from both HTS and low-temperature superconductors (LTS) will be used to illustrate suggested models. An important example is the unusual field-induced broadening of resistivity transitions, ρ(T,H), which places limitations on the value of the materials for moderate to high-field applications and has led to theories of thermally-activated magnetic flux creep[6], flux-lattice melting[7] or a vortex-glass transition[8]. Although the broadening looks similar[4] for the applied field, H, oriented *parallel* to the superconducting Cu-O layers (H||*ab*) or parallel to the *c*-axis (H||*c*), its width and the detailed shape of ρ(T,H) are different, as the proposed explanations which will be treated separately. These models also have implications to the low-temperature critical current density, J_c.

For H||*ab*, the broadening is smaller, and the absence of any measurable Lorentz-force dependence[2-4] together with the anticipated intrinsic pinning of the insulating region between layers, leads to an explanation of this dissipation which does not involve motion of vortices from the external field[4]. This Lorentz-force independence is also found[4] in the low-temperature J_c and the current-voltage characteristics, I(V), for *c*-axis-oriented films of $Tl_2Ba_2CaCu_2O_x$. The intrinsic pinning is also demonstrated in J_c measurements on multilayers[9] of the LTS superconductor NbN with insulating AlN. A crossover is observed from depinning of the external-field vortices at high fields to phase slips at intergranular Josephson junctions in the NbN layers at low fields: these phase slips do not require the existence of an external field.

For H||*c*, the lack of intrinsic pinning implies that the much greater broadening in HTS is due to thermally-activated flux motion. For the *highly-anisotropic* HTS, we show experimental evidence that the flux motion associated with this broaden-

*This work is supported by the U.S. Department of Energy, Basic Energy Sciences-Materials Sciences under contract #W-31-109-ENG-38, the National Science Foundation-Office of Science and Technology Centers under contract #STC8809854.

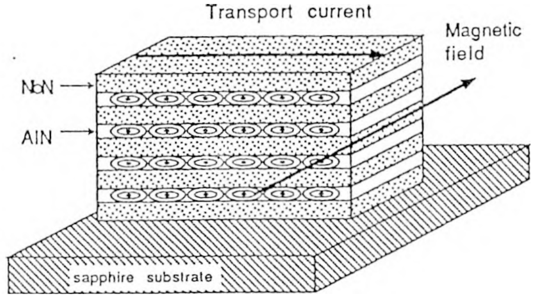

FIGURE 1
Configuration of magnetic field and transport current in an artificial multilayer of NbN/AlN.

ing occurs[10] as a result of a dimensional crossover from three dimensional (3D) vortex *lines* to 2D independent *pancake-like* vortices[11], which reside in well-coupled adjacent Cu-O bi- or tri-multilayers. This decoupling of vortices renders the sparse pinning sites in individual Cu-O multilayers to be much less effective. The 3D to 2D crossover is shown[10] to occur when k_BT exceeds the Josephson coupling energy of these Cu-O multilayers. For the less-anisotropic $YBa_2Cu_3O_7$, this dimensional crossover does not occur *below* H_{c2}, presumably because the conducting Cu-O chains short circuit[12] the Josephson interlayer coupling. The resulting 3D dissipation may be explained by thermally-activated magnetic flux creep[6] or a vortex-glass transition[8]. These results explain why $YBa_2Cu_3O_7$ has the best properties in a field and also shows that strong interlayer coupling is a key to finding good alternatives.

2. FIELD PARALLEL TO LAYERS

2.1. Crossover in NbN/AlN multilayers

Studies related to the intrinsic pinning of the Cu-O layers for fields parallel to them have been done in sputtered artificial multilayers of the LTS superconductor NbN with insulating AlN. The fabrication and characterization is discussed elsewhere[9]. The multilayer structure and measurement geometry are shown in Fig. 1, which also indicates that the magnetic vortices, which are shown projected onto the front side, lie in the

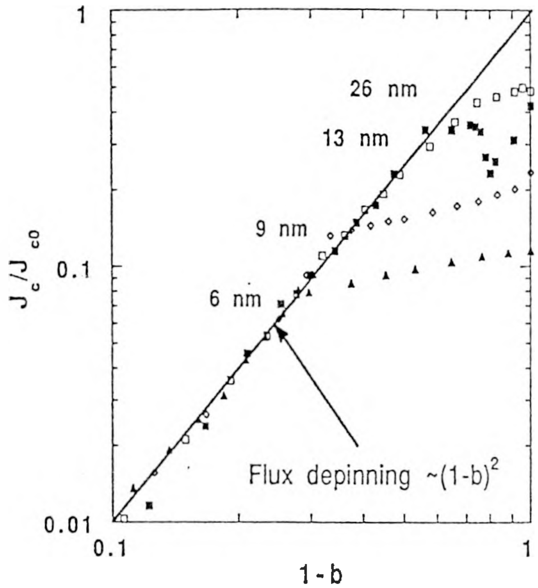

FIGURE 2
Normalized critical current density for various multilayers of NbN/AlN vs. reduced field.

strongly pinning AlN insulating layers (thickness of 2 nm). For the various NbN layer thicknesses shown in Fig. 2, in which T_c varied between 10 and 15 K, the field-dependent J_c at a temperature of 4.2 K is plotted against 1-b, where $b \equiv H/H_{c2}$. The high-field behavior is always a good fit to the $(1\text{-}b)^2$ dependence of vortex depinning from an ideal planar vacuum interface[13], but there is a sharp crossover at a reduced field which varies with NbN thickness. Further experiments, with the field rotated parallel to the transport current (see Fig. 1), tested the Lorentz-force dependence. As opposed to the high-field behavior, J_c was completely independent of the macroscopic Lorentz force at low-fields. To explain the low-field J_c, we recognized that the columnar grains in NbN sputtered films (10-100 nm diameter) are surrounded[14] by thin insulating boundaries which couple the superconducting grains by the Josephson effect. In these junctions, dissipation occurs by phase slips which have[15] a weaker field dependence than $(1\text{-}b)^2$ and no Lorentz-force dependence to satisfy the conditions for the low-field behavior shown in Fig. 2.

2.2. Intergranular Josephson junction model

In zero field, the Josephson critical current, I_{cj}, depends on the product of the superconducting order parameters, ψ_a and ψ_b, on each side of the junction[16]. Applied fields will be quite uniform for $\mu_o H > 0.2$ T, because then the penetration length, λ, is >> the flux line spacing, but depairing by the field will reduce ψ: Abrikosov's solution[17] of the vortex lattice determines the *spatial average* of ψ from $<\psi^2> = \psi_o^2(1\text{-}b)$, where ψ_o is the zero-field value. Thus to first order, $I_{cj} \propto \psi_a\psi_b \propto (1\text{-}b)$, which is a weaker field dependence than $(1\text{-}b)^2$ for pinning. However, because the flux cores (which account for the smallest ψ) are pinned in the AlN insulating layers, the *reduction* in I_{cj} between NbN grains will be smaller than the above, although still proportional to the vortex density (i.e., $I_{cj} \propto (1\text{-}\eta b)$, where $\eta < 1$), which is in agreement with the data of Fig. 2. In addition, statistical averaging of the complex, random geometry will smear out any interference effects which are small anyway, because the junctions are so small. Finally, Josephson phase slippage occurs in zero field and does not require flux motion of the external field, so it is independent of the macroscopic Lorentz force.

We interpret the data of Fig. 2 as a competition between depinning of the external field vortices and Josephson phase slippage with the experimental J_c measuring the weaker. For b less than the crossover field, b^*, the Josephson critical current between grains of the film is smaller than the depinning critical current, which is presumed to continue to increase as $(1\text{-}b)^2$ as in the single NbN films. For $I \perp H$, the Lorentz force is a maximum and there will be a crossover to depinning (at b^*), if $J_{cj} < J_{c0}$, because of the weaker field dependence of J_{cj}. Such a crossover is not expected for $I \parallel H$, and J_c is significantly larger (~3 times) than for $I \perp H$. For $I \parallel H$, J_c does not appear to follow the

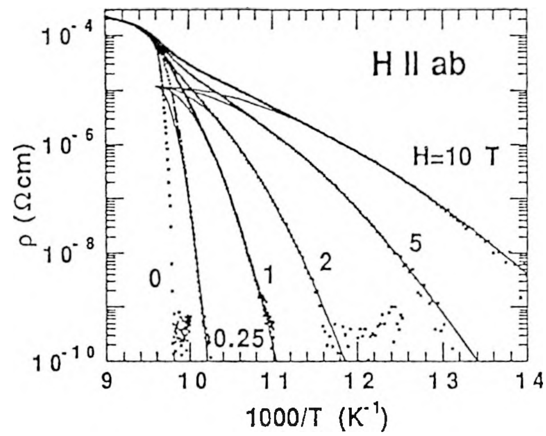

FIGURE 3
Resistive transitions in a c-axis oriented thin film of $Tl_2Ba_2CaCu_2O_x$ for fields parallel to the layers.

pure Josephson behavior up to H_{c2}, but rather a mixed behavior which can be understood as a residual Lorentz force due to possible inhomogeneous intergranular current paths.

2.3 Measurements in $Tl_2Ba_2CaCu_2O_x$

Sputtered films of $Tl_2Ba_2CaCu_2O_x$ were prepared and appropriately characterized[4]. Resistive transitions for H parallel to the Cu-O layers are shown in Fig. 3 for a current density of 10 A/cm^2. These results, as well as the low-temperature J_c and I(V), were shown to be strictly independent of the Lorentz force, and since significant intrinsic vortex pinning is expected from the wide insulator spacing between Cu-O bilayers, a mechanism other than vortex motion is suggested here[4], as in the NbN/AlN multilayers. We can rule out misalignment of the external field or crystal axes because an *average* value of 3.8° would be needed to explain the results. Likewise, the thermal generation of vortex/anti-vortex pairs cannot easily explain the large increase in broadening in very small fields compared to H_{c2}. Fitting this data of Fig. 3 is complicated by the 'double-transitions', which are very reminiscent of resistive transitions for granular materials[18] and two-dimensional Josephson junction[19] or proximity-coupled[20] superconducting arrays. In these cases, the superconducting grains or islands exhibit transitions at their T_c resulting in the initial resistance decrease, but not to zero resistance. The grains or islands then couple to each other with a supercurrent at a lower temperature. Thus we fit the lower-temperature transitions to:

$$\rho(T,H)=\rho_o \exp\left(\frac{-U(T,H)}{T}\right), \qquad (1)$$

where the activation energy, $U(T,H)$, is best fit[4] by the form $U_o(H)(1-t)^2$ where $t \equiv T/T_c$. We find fixed values of 1.2×10^{-5} Ωcm for ρ_o and 104.2 K for T_c (which should be virtually unaffected by H because H_{c2} is so large). This T_c is very close to the mean-field value of 104.6 K determined by fitting the resistance above T_c to the 2D fluctuation model[5]. The excellent agreement of the fit is shown in Fig. 3, and $U_o(H)=64500[K]/H^{1.09}$ is the only free parameter, with H in T. The measured low-temperature J_c was proportional to $(1-t)^2/H^{0.24}$.

Following the results in the NbN/AlN multilayers we try to fit the data to a classical Josephson junction with an insulator barrier, for which U is given[16] in zero field as E_{cj}/k_B, where

$$E_{cj} = \hbar I_{cj}/e, \qquad (2)$$

$$I_{cj}(T) = \frac{\pi\Delta(T)}{2eR_N} \tanh\left(\frac{\Delta(T)}{2k_BT}\right), \qquad (3)$$

where R_N is the normal-state junction resistance (e.g., above T_c) and $\Delta(T)$ is the energy gap. Using the above extension to finite fields, $U \propto (1-b)(1-t)$ near to T_c. These field and temperature dependences were confirmed by measurements in granular NbN films[15], but they are in conflict with the fits of Fig. 3 and the measured J_c. This temperature dependence can be resolved by recent measurements[21] on individual grain-boundary junctions in $YBa_2Cu_3O_7$ showing $I_c \sim (1-t)^2$. These have been interpreted as insulator junctions by applying the boundary conditions of Deutscher and

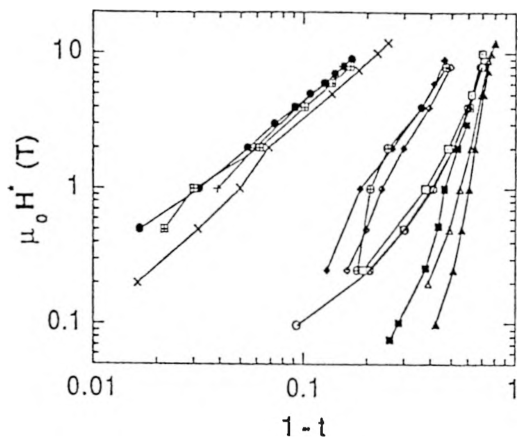

FIGURE 4
The characteristic fields for thermal activation for various HTS fall in four groups. From left, $YBa_2Cu_3O_7$; $TlBa_2CaCu_2O_x$ and $TlBa_2Ca_2Cu_3O_x$; $Tl_2Ba_2CaCu_2O_x$; and $Bi_2Sr_2CaCu_2O_x$. See text.

Müller[22]. Alternatively, normal-metal barrier proximity junctions[20,23] give this temperature dependence. However, the field dependence is hard to understand within a simple Josephson junction model, so the exact nature of the residual non-vortex motion dissipation in $Tl_2Ba_2CaCu_2O_x$ for H$\parallel$*ab* is still unclear.

3. FIELD PARALLEL TO *c*-AXIS

3.1. Thermal activation in HTS

For H$\parallel$c, the lack of intrinsic pinning implies that the much greater broadening is due to thermally-activated flux motion[6-8], which can be characterized experimentally by the resistivity transitions such that $\rho(T,H^*)/\rho_n = 10^{-5}$, where ρ_n is the extrapolated normal-state resistivity at T_c (e.g., see Fig. 4 of Ref. 4). These H^* are plotted in Fig. 4 against 1-t for many samples of five HTS, including some from the literature[24-26]. For the Bi- and Tl-systems, the data are inadequate to compare the magnetically-measured irreversibility line to H^*, but our thermally-activated model implies that agreement between these would depend on having equivalent sensitivities for internal electric fields in each measurement. Such an equivalence[27,28] is demonstrated explicitly for $YBa_2Cu_3O_7$ in Fig. 1, although the good agreement may be related to the existence of a vortex-glass phase transition[8], rather than equivalent sensitivities. Figure 1 also shows that H^* is fairly independent of sample quality (e.g., epitaxial or polycrystalline films, single crystals, minor amounts of second-phase material, etc.), at least with our uniform criteria. For $Tl_2Ba_2CaCu_2O_x$, the data for two *polycrystalline* and one *epitaxial* film coincide quite well, even though the measured J_c of the epitaxial film is ~10 times larger for all H and T. Deviations of the low-field data for $TlBa_2CaCu_2O_x$ and $TlBa_2Ca_2Cu_3O_x$ are likely an artifact due to minor impurity phases which nonetheless caused double-transitions *in that field range.* Note that the shape of $\rho(T,H)$ can vary from sample to sample perhaps due to the differences in their morphology. For example, the $YBa_2Cu_3O_7$ data in Fig. 1 bunch together, even though the single-crystal data exhibited a kink near the foot of the transition[25,27] which is not found in our epitaxial films.

3.2 Josephson interlayer coupling model

An important step for understanding these data was the recognition that weak coupling between superconducting Cu-O layers, implied by a high degree of anisotropy, allows for *thermally activated* decoupling of the magnetic-field-induced pancake-like[11] vortices in adjacent Cu-O layers, for H||c. The resulting independent motion of vortices in adjacent layers, i.e., two-dimensional (2D) behavior, greatly reduces the effectiveness of pinning (e.g., by point defects in the Cu-O layers), when compared to extended, 3D vortex *lines*. However, even in the 2D regime, *any* finite pinning strength in the individual Cu-O multilayers can become effective at sufficiently low temperatures, thereby increasing H^* above the dimensional crossover value. Since the experimental data indicate a weak dependence of H^* on sample quality even at low temperatures (for fields up to ~10 T), the most likely low-temperature processes, which will be considered below, are intrinsic flux-lattice melting or depinning from universal pinning sites, such as oxygen vacancies in the Cu-O layers. In the latter case, we envision enough elasticity in the flux lattice that individual vortices can be thermally depinned after which *another* vortex falls into the vacant potential well. Our uncertainty about the low-temperature mechanism, means we cannot rule out that additional pinning may increase H^* at low temperatures.

The dimensional crossover occurs when the coupling energy between adjacent Cu-O multilayers, $E_c(H,T)$, is ~k_BT. Previously, electromagnetic coupling of vortices was considered, but the relevant E_c was found[11] to be too small to explain the *relatively* narrow resistive transition in $YBa_2Cu_3O_7$, and it could hardly account for the vast differences found between $YBa_2Cu_3O_7$ and the highly-anisotropic HTS $Bi_2Sr_2CaCu_2O_x$ and $Tl_2Ba_2CaCu_2O_x$. On the other hand, the magnitude of the Josephson coupling energy, E_{cj}, for the *phase* of the superconducting order parameter[16], exhibits the right range of values in the highly-anisotropic HTS because ρ_c is so large. For Josephson tunneling through an insulating barrier, E_{cj} is given by Eqs. 2 and 3 *for zero magnetic field*, and must include the (1-b) term *for finite fields*, to account for the spatial average over the flux-line lattice. For Josephson coupling of a vortex to *both* neighboring Cu-O layers, $E_c=2E_{cj}$, and the relevant junction area is that of one vortex, Φ_o/H, so that $R_N=\rho_c s \mu_o H/\Phi_o$, where s is the repeat distance of the Cu-O multilayers. From standard tunneling theory[29] and experiment[30], R_N should be proportional to $\exp(-d_i/d_0)$, where d_i is the insulator thickness and $d_0=\hbar/\sqrt{8m\Phi}$ accounts for the tunneling barrier height, Φ. We always assume ρ_c is independent of T and H. The resulting 3D to 2D dimensional crossover is shown as the solid line in Fig. 5 for reasonably weak

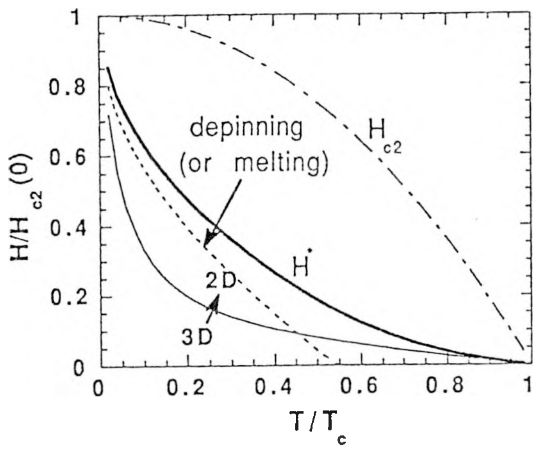

FIGURE 5
Characteristic fields for thermally-activated 3D to 2D crossover, flux depinning and the combined effect of both to produce H^*. Also shown is H_{c2}.

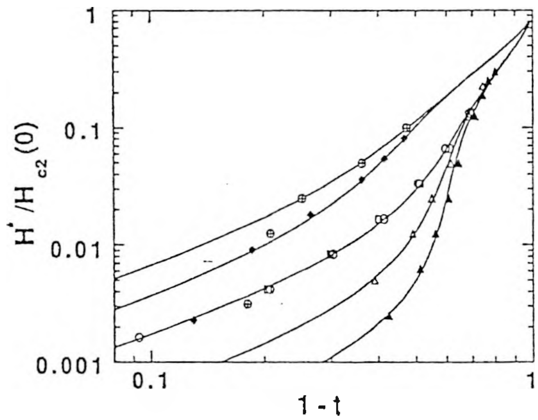

FIGURE 6
Data for H^* as defined in the text for various HTS, along with fits (solid lines) to the model. From top: $TlBa_2CaCu_2O_x$; $TlBa_2Ca_2Cu_3O_x$; several films of $Tl_2Ba_2CaCu_2O_x$; and two $Bi_2Sr_2CaCu_2O_x$ single crystals.

coupling, i.e., high anisotropy.

Flux-lattice melting in 2D occurs for $k_BT=E_m$, where[7]

$$E_m = \frac{A\, C_{66}\, \Phi_o\, d_s}{2\pi\, \mu_o H}, \tag{4}$$

where A is of order one, d_s is the superconducting Cu-O bi- or tri-layer thickness and the shear modulus has been determined by Brandt[31] to be:

$$C_{66} = \frac{B_c^2}{2\mu_o}\, b\,(1\text{-}0.29b)\,(1\text{-}b)^2, \tag{5}$$

where B_c is the thermodynamic critical field.

Alternatively, we consider depinning. The energy associated with depinning is given by that fraction, α, of the loss in superconducting condensation energy of a vortex line, which is compensated by a particular pinning site[13]:

$$E_p = \alpha\, \pi\xi_{ab}^2 d_s\, \frac{B_c^2}{2\mu_o}\, (1\text{-}b)^2. \tag{6}$$

For both $B_c(t)$ and $H_{c2}(t)$, we assume the clean-limit temperature dependence of $1\text{-}t^2$, which has some justification from measurements[32] in $YBa_2Cu_3O_7$. In that case, the ratio of these, i.e., $E_p/E_m=2\pi\alpha(1+t)/A(1\text{-}0.29b)$, is weakly dependent on b and t, so that both terms give reasonable fits to the data when combined with the Josephson tunneling model and it is not possible to choose between them based on the present data and analysis. An example of thermally-activated depinning is also shown in Fig. 5 as a dashed line for the parameters $\alpha\Phi_o d_s B_c(0)^2/4\mu_o k_B T_c B_{c2}(0)=0.5$ and $[\pi\hbar\Phi_o/e^2\rho_c s B_{c2}(0)]\,[\Delta(0)/k_BT_c]=0.05$. It should be noted that $E_p=k_BT$ always has a solution with $b=H^*/H_{c2}=0$ and a finite $T<T_c$. This can be seen from Eq. 6 and the same is true for E_m. However, extending these solutions into the 3D regime at low fields would be incorrect since it would not describe vortex *line* interactions, whereas the distinction between 2D and 3D is valid even at the lowest temperatures. For vortices to move, they must overcome *both* energy barriers, so we fit the H^* data by solving $k_BT=E_p(H,T)+2E_{cj}(H,T)$, as shown in Fig. 5 as the heavy solid line.

3.3 Results and implications

The data of Fig. 4 are thus fit using three parameters: H_{c2}; ρ_c, which is related to the strength of Josephson coupling; and $\alpha B_c^2/2\mu_o$, which is related to the pinning strength (or a similar parameter for a melting transition). Assuming the BCS value of 1.76 for $\Delta(0)/k_BT_c$, these fits are shown in Fig. 6 and the resulting parameters are given in Table I together with other *derived* ones. The values of $B_c(0)$ assume that α=1, κ is given by $\mu_oH_{c2}(0)/\sqrt{2}B_c(0)$, and $H_{c1}(0)$ is $B_c(0)\ ln(\kappa)\ /\sqrt{2}\kappa$. The coherence lengths are given by $\xi_{ab}(0)=\sqrt{\Phi_o/2\pi\mu_oH_{c2}(0)}$ and $\lambda_{ab}(0)=\kappa\ \xi_{ab}(0)$. An important further prediction of coupling by Josephson tunneling is an exponential dependence of ρ_c on d_i, and the data are shown in Fig. 7 for the Tl- and Bi-based HTS materials. While these data do not fall on one straight line, we anticipate the possibility of different tunneling barrier heights or tunneling effective masses, at least between Bi-O and Tl-O insulating layers. Nevertheless, the best fit gives a reasonable value of d_o=1 Å and a barrier height of 0.8 eV assuming a free electron mass. Values of d_o=1-1.6 Å are typically found in artificial or natural oxide tunneling barriers[29,30].

The derived parameters presented in Table I should be viewed with some caution because of our somewhat arbitrary criterion for H^*, uncertainty over the proper low-temperature model of flux dynamics and our untested, but reasonable, clean-limit assumption that $B_c(t)$ and $H_{c2}(t)$ are proportional to $1\text{-}t^2$. In addition, in some cases the data do not span a sufficient field range to tie down the parameters of the fits precisely. Nonetheless, the

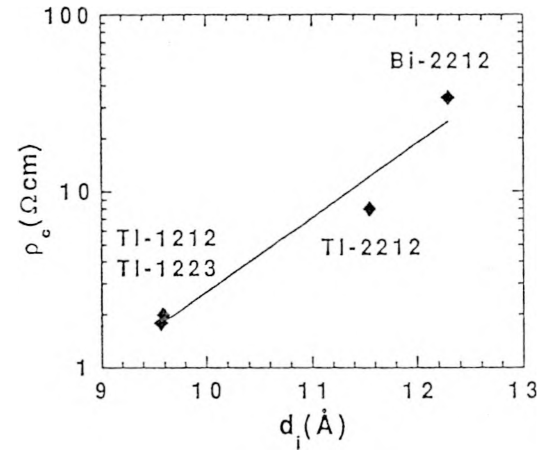

FIGURE 7
Values of ρ_c for the fits of Fig. 6 indicating the exponential dependence on the Cu-O multilayer spacing d_i, expected for Josephson tunneling.

parameters are reasonable. In particular, the penetration length, $\lambda_{ab}(0)$, and $B_c(0)$ are close to expectations based on measured values for $YBa_2Cu_3O_7$ of[32] 140 nm and[33] ~0.8 T, respectively. For $Bi_2Sr_2CaCu_2O_x$, recent muon spin-resonance experiments[34] have concluded that $\mu_oH_{c2}(0)$=44 T, κ~100 and λ_{ab}~250 nm, in good agreement with Table I.

A further prediction of this model is that *dimensional crossover* is independent of the pinning strength, whereas the low-temperature H^*, and particularly J_c, can be enhanced by

Table I. Parameters for the highly-anisotropic HTS studied in this paper. Structural data come from the literature and T_c is measured directly. The fits shown in Fig. 6 provide $H_{c2}(0)$, ρ_c and $\alpha B_c(0)^2$, while the rest are derived from formulas in the text assuming α=1.

Sample	s (Å)	d_i (Å)	d_s (Å)	T_c (K)	$\mu_0H_{c2}(0)$ (T)	ρ_c (Ωcm)	$\alpha B_c(0)^2/2\mu_0$ (J/cm³)	$B_c(0)$ (T)	κ	$\mu_0H_{c1}(0)$ (T)	$\xi_{ab}(0)$ (Å)	$\lambda_{ab}(0)$ (Å)
Tl-1212	12.75	9.57	3.18	72	80	1.8	0.11	0.53	110	0.0165	20	2100
Tl-1223A	15.87	9.59	6.28	104	110	2	0.13	0.56	140	0.0141	17	2400
Tl-2212	14.7	11.55	3.15	100	60	8	0.087	0.47	91	0.0164	23	2100
Bi-2212A	15.45	12.29	3.16	80	40	34	0.049	0.35	81	0.0135	28	2300
Bi-2212B	15.45	12.29	3.16	79	40	84	0.047	0.34	82	0.0130	28	2300

improved flux pinning: evidence for this is found in the $Tl_2Ba_2CaCu_2O_x$ films reported above, proton-irradiated $YBa_2Cu_3O_7$ crystals[28], an alpha-irradiated $Bi_2Sr_2CaCu_2O_x$ single crystal[1] and[35] neutron-irradiated $Tl_2Ba_2Ca_2Cu_3O_x$ polycrystals. These studies report small changes at low temperatures in the irreversibility line or resistive tail, but large differences in J_c.

The data for $YBa_2Cu_3O_7$ could not be fit to the model with a reasonable value of ρ_c: a possible explanation is that the electrically conducting[12] Cu-O chains short circuit the tunneling between adjacent Cu-O bilayers in $YBa_2Cu_3O_7$, yielding a much lower anisotropy and ρ_c. Thus for the smaller experimental ρ_c for $YBa_2Cu_3O_7$, the model predicts the dimensional crossover to be *above* $H_{c2}(T)$ and our model does not treat the dynamics of 3D vortex lines. Information based largely on the current-voltage characteristics, I(V), tends to support[36] a picture of a vortex glass transition for $YBa_2Cu_3O_7$. For $Tl_2Ba_2CaCu_2O_x$, the I(V) for a similar range of parameter space *do not* support[4] such a vortex glass model.

3. SUMMARY OF CONCLUSIONS

The dissipation associated with the broadened resistive transitions of the highly-anisotropic high-temperature superconductors has been studied for fields parallel and perpendicular to the superconducting layers. The absence of any Lorentz force for H parallel to the Cu-O layers is shown, by analogy with artifical multilayers of superconducting NbN with insulating AlN, to be due to the strong intrinsic pinning of the layered structure, such that the residual measured dissipation is due to a mechanism not involving vortex motion. For H perpendicular to the Cu-O layers, vortex motion causes the dissipation, but only after a crossover from 3D vortex lines to 2D vortex pancakes. This intrinsic crossover is determined by the Josephson coupling between Cu-O bi- or tri-layers and thus is unaffected by additional flux pinning. At low temperatures, pinning can be effective even in the uncoupled 2D layers, and can also increase H^* and the critical current density in this model.

ACKNOWLEDGEMENTS

This research was done in collaboration with R.T. Kampwirth, J.M. Murduck, D.M. McKay, K.C. Woo, S.J. Stein, J.C. Smith, D.S. Richeson, T.J. Marks, J.H. Kang, J. Talvacchio, M. Eddy, D. Hampshire, R. Herzog and H.W. Weber.

REFERENCES

1. T.T.M. Palstra, B. Batlogg, L.F. Schneemeyer and J.V. Waszczak, submitted to *Phys. Rev.* B43, 3756 (1991).
2. Y. Iye, S. Nakamura and T. Tamegai, *Physica* C159, 433 (1989); K. Kitazawa, S. Kambe, M. Naito, I. Tanaka and H. Kojima, *Japan. J. Appl. Phys.* 28, L555 (1989); H. Iwasaki, N. Kobayashi, M. Kikuchi, T. Kajitani, Y. Syono, Y. Muto and S. Nakajima, *Physica* C159, 301 (1989).
3. K.C. Woo, K.E. Gray, R.T. Kampwirth, J.H. Kang, S.J. Stein, R. East and D.M. McKay, *Phys. Rev. Lett.* 63, 1877 (1989).
4. D.H. Kim, K.E. Gray, R.T. Kampwirth and D.M. McKay, *Phys. Rev.* B42, 6249 (1990).
5. D.H. Kim, A.M. Goldman, J.H. Kang, R.T. Kampwirth and K.E. Gray, *Phys. Rev.* B39, 12275 (1989).
6. P.H. Kes, J. Aarts, J. van den Berg, C.J. van der Beek and J.A. Mydosh, *Supercond. Sci. Technol.* 1, 242 (1989).
7. J.M. Kosterlitz and D.J. Thouless *J. Phys.* C6, 1181 (1973); B.A. Huberman and S. Doniach, *Phys. Rev. Lett.* 43, 950 (1979).
8. M.P.A. Fisher, *Phys. Rev. Lett.* 62, 1415 (1989).
9. K.E. Gray, R.T. Kampwirth, D.J. Miller, J.M. Murduck, D. Hampshire, R. Herzog and H.W. Weber, *Physica* C174, 340 (1991).

10. D.H. Kim, K.E. Gray, R.T. Kampwirth, J.C. Smith, D.S. Richeson, T.J. Marks, J.H. Kang, J. Talvacchio and M. Eddy, to be published.

11. J.R. Clem, *Phys. Rev.* **B43**, 7837 (1991).

12. U. Welp, S. Fleshler, W.K. Kwok, J. Downey, Y. Fang, G.W. Crabtree and J.Z. Liu, *Phys. Rev.* **B42**, 10189 (1991).

13. K.E. Gray, R.T. Kampwirth, J.M. Murduck and D.W. Capone II, *Physica* **C152**, 445 (1988).

14. H.L. Ho, R.T. Kampwirth, K.E. Gray, D.W. Capone II and L.S. Chumbley, *Ultramicroscopy* **22**, 297 (1987).

15. D.H. Kim, K.E. Gray, R.T. Kampwirth, K.C. Woo, D.M. McKay and J. Stein, *Phys. Rev.* **B41**, 11642 (1990).

16. P.W. Anderson, Lectures at Ravello Spring School, 1963; V. Ambegaokar and A. Baratoff, *Phys. Rev. Lett.* **10**, 486 (1963).

17. A.A. Abrikosov, *Zh. Eksperim. i Teor. Fiz.* **32**, 1442 (1957); *Soviet Phys. JETP* **5**, 1174 (1957), and also A.L. Fetter and P.C. Hohenberg, in Superconductivity, edited by R.D. Parks, (Marcel Dekker, New York, 1969), p.851.

18. S.A. Wolf, D.U. Gubser, W.W. Fuller, J.C. Garland and R.S. Newrock, *Phys. Rev. Lett.* **47**, 1071 (1981).

19. R.F. Voss and R.A. Webb, *Phys. Rev.* **25**, 3446 (1982).

20. D.J. Resnick, J.C. Garland, J.T. Boyd, S. Shoemaker and R.S. Newrock, *Phys. Rev. Lett.* **47**, 1542 (1981); D.W. Abraham, C.J. Lobb, M. Tinkham and T.M. Klapwijk, *Phys. Rev.* **26**, 5268 (1982).

21. R. Gross, P. Chaudhari, D. Dimos, A. Gupta and G. Koren, *Phys. Rev. Lett.* **64**, 228 (1990).

22. D. Deutscher and K.A. Müller, *Phys. Rev. Lett.* **59**, 1745 (1987).

23. P.G. de Gennes, *Rev. Mod. Phys.* **36**, 225 (1964).

24. T.T.M. Palstra, B. Batlogg, L.F. Schneemeyer and J.V. Waszczak, *Phys. Rev. Lett.* **61**, 1662 (1988).

25. T.T.M. Palstra, B. Batlogg, R.B. van Dover, L.F. Schneemeyer and J.V. Waszczak, *Appl. Phys. Lett.* **54**, 763 (1989).

26. W.K. Kwok, (private communication).

27. Y. Xu, M. Suenaga, Y. Gao, J.E. Crow and N.D. Spencer, *Phys. Rev.* **B42**, 8756 (1990).

28. L. Civale, A.D. Marwick, M.W. McElfresh, T.K. Worthington, A.P. Malozemoff, F.H. Holtzberg, J.R. Thompson and M.A. Kirk, *Phys. Rev. Lett.* **65**, 1164 (1990).

29. See e.g., E.L. Wolf, Principles of Electron Tunneling Spectroscopy (Oxford Univ. Press, New York, 1985).

30. K.E. Gray, *Solid State Commun.* **13**, 1787 (1973).

31. E.H. Brandt, *Phys. Status Solidi* **B77**, 551 (1976).

32. U. Welp, W.K. Kwok, G.W. Crabtree, K.G. Vandervoort and J.Z. Liu, *Phys. Rev. Lett.* **62**, 1908 (1989) and A. Umezawa, G.W. Crabtree, U. Welp, W.K. Kwok, K.G. Vandervoort and J.Z. Liu, *Phys. Rev.* **B42**, 8744 (1990).

33. L. Krusin-Elbaum, R.L. Greene, F. Holtzberg, A.P. Malozemoff and Y. Yeshurun, *Phys. Rev. Lett.* **62**, 217 (1989).

34. D.R. Harshman, R.N. Kleinman, M. Inui, G.P. Espinoza, D.B. Mitzi, A. Kapitulnik, D.L. Williams, *Bull. Am. Phys. Soc.* **36**, 470 (1991).

35. M.P. Maley, P.H. Kes, G.J. Vogt, D.S. Phillips andM.E. McHenry, *Bull. Am. Phys. Soc.* **36**, 984 (1991).

36. R.H. Koch, V. Foglietti, W.J. Gallagher, G. Koren, A. Gupta and M.P.A. Fisher, *Phys. Rev. Lett.* **63**, 1511 (1989) and P.L. Gammel, L.F. Schneemeyer and D.J. Bishop, *Phys. Rev. Lett.* **66**, 953 (1991).